

Remanence enhanced $\text{Nd}_2\text{Fe}_{14}\text{B}/\alpha\text{-Fe}$ and $\text{Nd}(\text{Fe}, \text{Mo})_{12}\text{N}_x/\alpha\text{-Fe}$ type magnetic powders produced by high-energy ball-milling

M. Jurczyk

CSIRO Division of Applied Physics, Lindfield, NSW 2070, Australia

Received 27 October 1995

Abstract

$\text{Nd}_{12.6}\text{Fe}_{81.4-y-z}\text{Co}_y\text{Zr}_z\text{B}_6$ (2:14:1 phase)/ $\alpha\text{-Fe}$ ($y=0$ or 11.6 and $z=0$ or 0.5) and $\text{Nd}_{12}\text{Fe}_{75}\text{Mo}_{13}\text{N}_x$ (1:12 phase)/ $\alpha\text{-Fe}$ powders, with a volume fraction of magnetically soft $\alpha\text{-Fe}$ phase up to 75%, have been prepared by a high-energy ball-milling and annealing, and in the case of the latter, nitrogenation. Enhanced remanent magnetic polarizations of 1.14 T and 0.85 T were obtained in $\text{Nd}_{12.6}\text{Fe}_{69.3}\text{Co}_{11.6}\text{Zr}_{0.5}\text{B}_6/\alpha\text{-Fe}$ and $\text{Nd}_{12}\text{Fe}_{75}\text{Mo}_{13}\text{N}_x/\alpha\text{-Fe}$ powders, with a volume fraction of magnetically soft $\alpha\text{-Fe}$ phase of around 40% respectively.

Keywords: Remanence enhanced materials; $\text{Nd}_2(\text{Fe}, \text{Co}, \text{Zr})_{14}\text{B}/\alpha\text{-Fe}$; $\text{Nd}(\text{Fe}, \text{Mo})_{12}\text{N}_x/\alpha\text{-Fe}$

1. Introduction

In the absence of intercrystalline exchange coupling, the remanent magnetic polarization J_r of an isotropic magnetic material consisting of a random array of magnetic particles, exhibiting uniaxial magnetocrystalline anisotropy, should equal one half of the saturation magnetic polarization J_s , i.e. the reduced remanent magnetic polarization $\alpha = J_r/J_s = 0.5$. Recent studies have reported significantly higher values of J_r , and hence values of α greater than 0.5, in nanocomposite two-phase mixtures consisting of magnetically hard and soft phases [1–5]. Modelling of hysteresis curves of isotropic nanocrystalline permanent magnet powders by Kneller and Hawig [2], Schrefl et al. [6], and Skomski [7], have shown that the coercivity and enhancement of remanent magnetic polarization are highly dependent on the grain size of the soft magnetic phase. In order to achieve a significant enhancement of J_r , and to preserve a high intrinsic coercivity in isotropic nanocrystalline $\text{Nd}_2\text{Fe}_{14}\text{B}$ -based magnets, a mean grain size of less than 20 nm is required [6].

New magnetic materials with enhanced remanent magnetic polarization were first reported by Coehoorn et al. [1] for isotropic melt-spun ribbons of $\text{Nd}_2\text{Fe}_{14}\text{B}$ and Fe_3B . Hirose et al. [3] produced a range of NdFe_3B -type alloys and showed that the addition of 3

to 5 at.% Co and a small quantity of Al, Si, Cu, Ga, Ag or Au improved the intrinsic coercivity and squareness of the hysteresis loop. Manaf et al. [4] described a new type of Nd-poor permanent magnet alloy based on NdFeB containing 8–9 at.% Nd, with a remanent magnetic polarization of 1.1 T, an intrinsic coercivity of 485 kA m^{-1} and an energy product of 158 kJ m^{-3} . Recently, Gong et al. [5] have produced mechanically alloyed $(\text{Nd,Tb})_2\text{Fe}_{14}\text{B}/(\text{FeCo,FeNb})$ powders with an enhanced remanent magnetic polarization in the range 0.9 to 1.0 T, reduced remanent magnetic polarization α of 0.60 to 0.68, and, intrinsic coercivity of 320 to 475 kA m^{-1} . Significant improvements in the intrinsic coercivity have been obtained with the addition of niobium to $\text{Nd}_2\text{Fe}_{14}\text{B}/\alpha\text{-Fe}$, owing to a reduction in the crystal grain size of the soft phase [5].

In this work Nd-poor $\text{Nd}_2(\text{Fe,Co,Zr})_{14}\text{B}$ and $\text{Nd}(\text{Fe,Mo})_{12}\text{N}_x$ nanocomposite powders are produced by high-energy ball-milling (HEBM) and annealing, and in the case of the latter, nitrogenation. The effect of the partial substitution of Fe by Co and Zr on the magnetic properties of $\text{Nd}_2\text{Fe}_{14}\text{B}/\alpha\text{-Fe}$ powders is investigated.

2. Materials preparation and structure

Alloy lumps of $\text{Nd}_{12.6}\text{Fe}_{81.4-y-z}\text{Co}_y\text{Zr}_z\text{B}_6$ ($y=0$,

11.6; $z = 0, 0.5$) and $\text{Nd}_{12}\text{Fe}_{75}\text{Mo}_{13}$ were prepared by arc melting stoichiometric amounts of the constituent elements (purity 99.9 at.% or better) in an argon atmosphere. Alloy of nominal composition $\text{Nd}_{12.6}\text{Fe}_{81.4}\text{B}_6$ was also purchased from Rare – Earth Products Ltd. Before HEBM the alloy lumps were crushed in an agate mortar to a particle size of less than 106 μm . The remanence enhanced powders were prepared by HEBM of the rare-earth containing powder and Fe powder (purity 99.9 at.% from Aldrich Chemical Company Inc., particle size not above 10 μm) in a SPEX 8000 Mixer Mill. The as-milled powders were heat treated in the temperature range 600–850 $^\circ\text{C}$ for 30 min under high purity argon to form either the $\text{NdFeB}(2:14:1)$ or $\text{NdFeMo}(1:12)$ phase respectively. The nitrides were prepared by nitrogeneration of $\text{Nd}(\text{Fe},\text{Mo})_{12}/\alpha\text{-Fe}$ powders at 450 $^\circ\text{C}$ for 25 h using 100 kPa pressure of nitrogen.

The powders were examined by XRD analysis, using $\text{Cu K}\alpha$ radiation, and the mean grain size of the powders was determined from X-ray line broadening using the Scherrer formula [8].

2.1. $\text{Nd}_2(\text{Fe},\text{Co},\text{Zr})_{14}\text{B}/\alpha\text{-Fe}$ type materials

Fig. 1(A) shows XRD patterns of HEBM powders based on 60 vol.% $\text{Nd}_{12.6}\text{Fe}_{69.3}\text{Co}_{11.6}\text{Zr}_{0.5}\text{B}_6$ and 40 vol.% $\alpha\text{-Fe}$, milled for 48 h and annealed. After HEBM the $\text{Nd}_{12.6}\text{Fe}_{69.3}\text{Co}_{11.6}\text{Zr}_{0.5}\text{B}_6$ alloy has decomposed into an amorphous phase and nanocrystalline $\alpha\text{-Fe}$ with a grain size of about 11 nm (Fig. 1(A)a). Heat treatment in high purity argon at 630 $^\circ\text{C}$ for 30 min results in the formation of the tetragonal $\text{Nd}_2\text{Fe}_{14}\text{B}$ -type phase (Fig. 1(A)b) which coexists with the $\alpha\text{-Fe}$ phase, forming a two-phase nanocomposite material. The grain size of the magnetically soft $\alpha\text{-Fe}$ phase after this heat treatment increased to around 35 nm (see Fig. 2).

2.2. $\text{Nd}(\text{Fe},\text{Mo})_{12}\text{N}_x/\alpha\text{-Fe}$ type materials

Fig. 1(B) shows XRD patterns of HEBM powders on 60 vol.% $\text{Nd}_{12}\text{Fe}_{75}\text{Mo}_{13}$ and 40 vol.% $\alpha\text{-Fe}$, milled for 47 h, annealed and nitrogenerated. After HEBM the $\text{Nd}_{12}\text{Fe}_{75}\text{Mo}_{13}$ alloy has decomposed into an amorphous phase and nanocrystalline $\alpha\text{-Fe}$ with a fine grain size of about 15 nm (Fig. 1(B)a). Heat treatment in high purity argon at 730 $^\circ\text{C}$ results in the formation of the tetragonal ThMn_{12} -type phase (Fig. 1(B)b), which coexists with $\alpha\text{-Fe}$, with an average grain size of about 45 nm. At this stage the material is still magnetically soft due to the magnetic in-plane anisotropy of the $\text{Nd}(\text{Fe},\text{Mo})_{12}$ phase. Subsequent annealing in a high purity nitrogen atmosphere at 450 $^\circ\text{C}$ for 25 h results in a lattice expansion of ThMn_{12} -type phase of about 3% (Fig. 1(B)c). This process induces hard magnetic

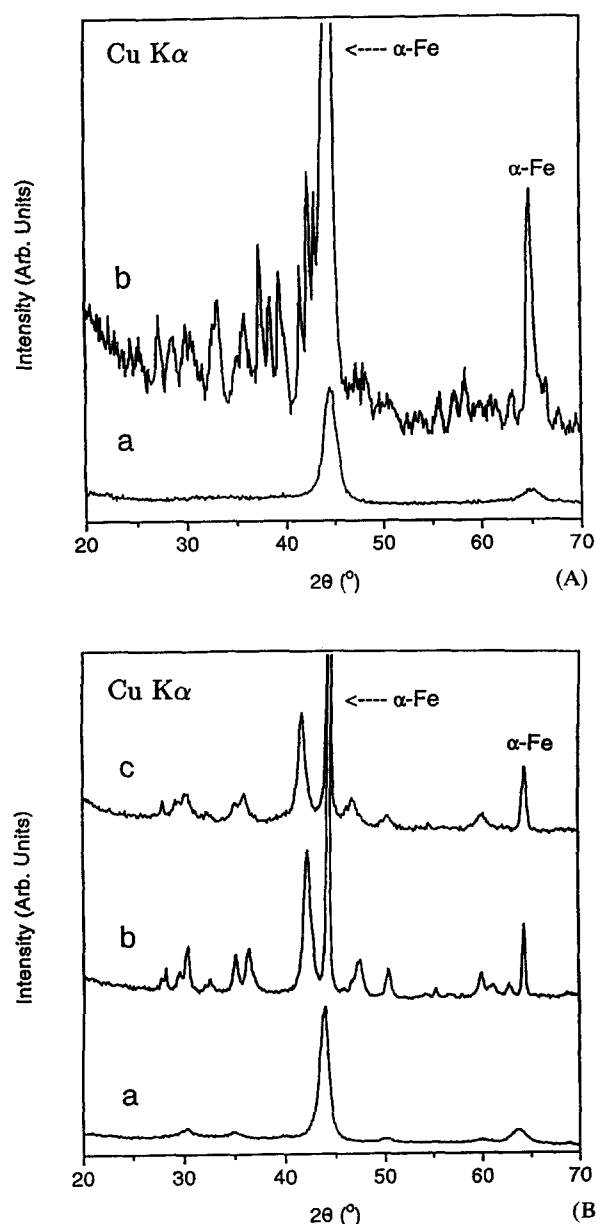


Fig. 1. XRD spectra of (A) $\text{Nd}_{12.6}\text{Fe}_{69.3}\text{Co}_{11.6}\text{Zr}_{0.5}\text{B}_6/\alpha\text{-Fe}$ powders with a volume fraction of magnetically soft $\alpha\text{-Fe}$ phase of 40%, (a) high-energy ball-milled for 48 h, and (b) heat treated at 630 $^\circ\text{C}$ for 30 min, $\text{Cu K}\alpha$ radiation was used; (B) $\text{Nd}_{12}\text{Fe}_{75}\text{Mo}_{13}\text{N}_x/\alpha\text{-Fe}$ powders with a volume fraction of magnetically soft $\alpha\text{-Fe}$ phase of 40%, (a) high-energy ball-milled for 47 h, (b) heat treated at 730 $^\circ\text{C}$ for 30 min, and (c) nitrogenerated at 450 $^\circ\text{C}$ for 25 h.

properties, as the magnetic anisotropy switches from being in-plane to uniaxial. Annealing also increases the grain size of the magnetically soft $\alpha\text{-Fe}$ phase to around 57 nm (see Fig. 2).

3. Magnetic properties

Samples for the measurement of magnetic properties were made by mixing the powders with epoxy resin in suitable moulds in an applied magnetic field of

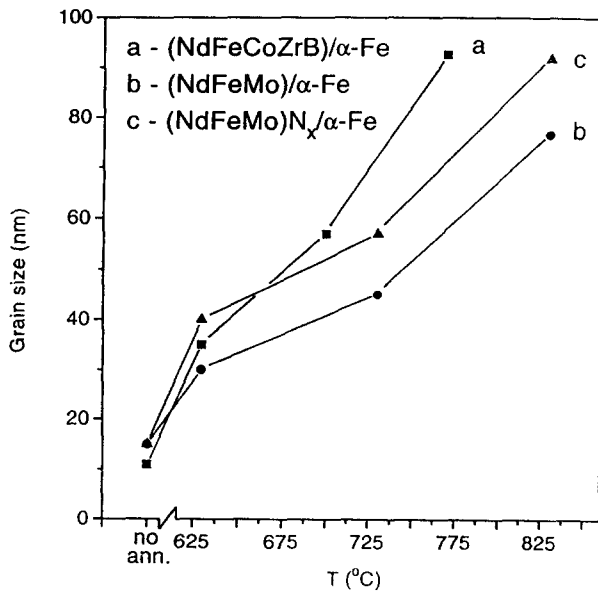


Fig. 2. The grain size of high energy ball milled (a) $\text{Nd}_{12.6}\text{Fe}_{69.3}\text{Co}_{11.6}\text{Zr}_{0.5}\text{B}_6/\alpha\text{-Fe}$, (b) $\text{Nd}_{12}\text{Fe}_{75}\text{Mo}_{13}/\alpha\text{-Fe}$, and (c) $\text{Nd}_{12}\text{Fe}_{75}\text{Mo}_{13}\text{N}_x/\alpha\text{-Fe}$ powders without annealing and after heat treatment at different temperatures, and in the case of (c) nitrogenation (in all cases the volume fraction of magnetically soft $\alpha\text{-Fe}$ phase is 40%; lines are provided as a guide to the eye).

1.6 Ma m^{-1} . The magnetic hysteresis curves were measured at room temperature using a vibrating sample magnetometer (VSM) and/or a Quantum Design SQUID magnetometer. The saturation magnetic polarization was determined in an applied field of 4 MA m^{-1} . All the powders were magnetically isotropic, and the intrinsic magnetic properties of a selection of HEBM $\text{Nd}_2(\text{Fe,Co,Zr})_{14}\text{B}/\alpha\text{-Fe}$ and $\text{Nd}(\text{Fe,Mo})_{12}\text{N}_x/\alpha\text{-Fe}$ powders are given in Table 1.

The intrinsic coercivity JH_c and the reduced remanent magnetic polarization α of $\text{Nd}_{12.6}\text{Fe}_{69.3}\text{Co}_{11.6}\text{Zr}_{0.5}\text{B}_6/\alpha\text{-Fe}$ powders with a volume fraction of magnetically soft $\alpha\text{-Fe}$ phase of 40%, as a function of annealing temperature for 30 min anneal, are shown in Fig. 3. A maximum intrinsic coercivity of 478 kA m^{-1} is obtained at an annealing temperature

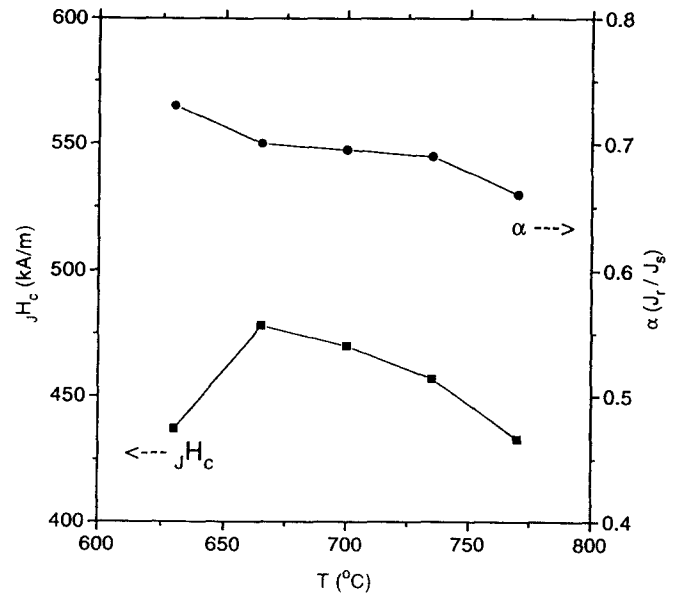


Fig. 3. The variation of the intrinsic coercivity JH_c and reduced remanent magnetic polarization $\alpha = J_r/J_s$ with annealing temperature for the $\text{Nd}_{12.6}\text{Fe}_{69.3}\text{Co}_{11.6}\text{Zr}_{0.5}\text{B}_6/\alpha\text{-Fe}$ powders with a volume fraction of magnetically soft $\alpha\text{-Fe}$ phase of 40% (lines are provided as a guide to the eye).

of 665°C . JH_c is lower in powders annealed at both lower and higher temperatures, as the grain size of the soft $\alpha\text{-Fe}$ phase is either too small or too large for optimum exchange coupling. The reduced remanent magnetic polarization decreases from 0.73 to 0.66 as the annealing temperature increases. The maximum intrinsic coercivity of $\text{Nd}_{12.6}\text{Fe}_{69.3}\text{Co}_{11.6}\text{Zr}_{0.5}\text{B}_6/\alpha\text{-Fe}$ powder with a volume fraction of magnetically soft $\alpha\text{-Fe}$ phase of 40% is 478 kA m^{-1} , which compares with 680 kA m^{-1} reported earlier [9] for HEBM single 2:14:1 phase $\text{Nd}_{12.6}\text{Fe}_{69.3}\text{Co}_{11.6}\text{Zr}_{0.5}\text{B}_6$ powder.

The intrinsic coercivity and reduced remanent magnetic polarization of the $\text{Nd}_{12}\text{Fe}_{75}\text{Mo}_{13}\text{N}_x/\alpha\text{-Fe}$ powders, with a volume fraction of magnetically soft $\alpha\text{-Fe}$ phase of 40%, heat treated at $630\text{--}830^\circ\text{C}$ for 30 min and subsequently nitrogenated, are shown in Fig. 4. A maximum JH_c of 281 kA m^{-1} is obtained after heat

Table 1

Saturation magnetic polarization J_s , remanent magnetic polarization J_r , reduced remanent magnetic polarization α , and intrinsic coercivity JH_c at room temperature of some HEBM $\text{Nd}_2\text{Fe}_{14}\text{B}/\alpha\text{-Fe}$ and $\text{Nd}(\text{Fe,Mo})_{12}\text{N}_x/\alpha\text{-Fe}$ powders

| Material | Volume fraction of magnetically soft $\alpha\text{-Fe}$ phase (%) | J_s (T) | J_r (T) | α (J_r/J_s) | JH_c (kA m^{-1}) |
|--|---|-----------|-----------|------------------------|-------------------------------|
| $\text{Nd}_{12.6}\text{Fe}_{81.4}\text{B}_6/\alpha\text{-Fe}$ | 0 | 1.04 | 0.58 | 0.56 | 565 |
| $\text{Nd}_{12.6}\text{Fe}_{81.4}\text{B}_6/\alpha\text{-Fe}$ | 37.5 | 1.46 | 0.63 | 0.43 | 160 |
| $\text{Nd}_{12.6}\text{Fe}_{69.3}\text{Co}_{11.6}\text{Zr}_{0.5}\text{B}_6/\alpha\text{-Fe}$ | 0 | 0.96 | 0.67 | 0.70 | 680 |
| $\text{Nd}_{12.6}\text{Fe}_{69.3}\text{Co}_{11.6}\text{Zr}_{0.5}\text{B}_6/\alpha\text{-Fe}$ | 31 | 1.55 | 1.10 | 0.71 | 540 |
| $\text{Nd}_{12.6}\text{Fe}_{69.3}\text{Co}_{11.6}\text{Zr}_{0.5}\text{B}_6/\alpha\text{-Fe}$ | 37.5 | 1.62 | 1.14 | 0.70 | 504 |
| $\text{Nd}_{12.6}\text{Fe}_{69.3}\text{Co}_{11.6}\text{Zr}_{0.5}\text{B}_6/\alpha\text{-Fe}$ | 50 | 1.73 | 1.11 | 0.64 | 440 |
| $\text{Nd}_{12}\text{Fe}_{75}\text{Mo}_{13}\text{N}_x/\alpha\text{-Fe}$ | 0 | 0.77 | 0.42 | 0.55 | 716 |
| $\text{Nd}_{12}\text{Fe}_{75}\text{Mo}_{13}\text{N}_x/\alpha\text{-Fe}$ | 40 | 1.37 | 0.85 | 0.62 | 281 |

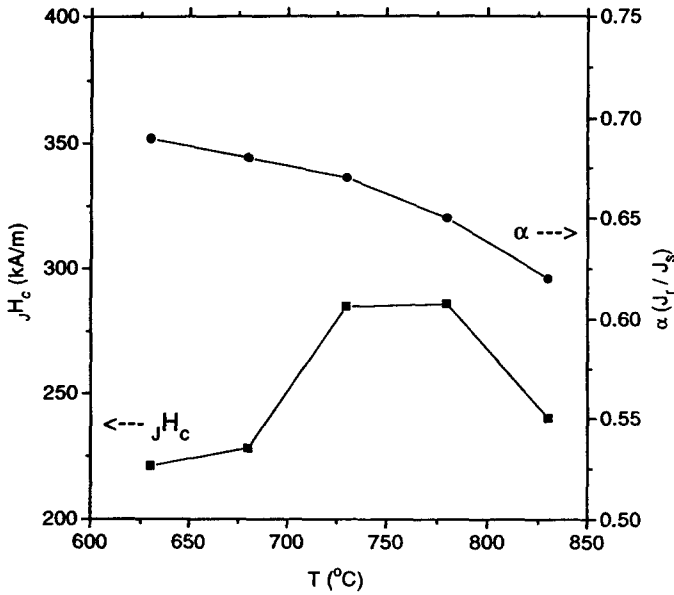


Fig. 4. The variation of the intrinsic coercivity jH_c and reduced remanent magnetic polarization $\alpha = J_r/J_s$ with annealing temperature prior to nitrogeneration for the $Nd_{12}Fe_{75}Mo_{13}N_x/\alpha-Fe$ powders with a volume fraction of magnetically soft $\alpha-Fe$ phase of 40% (lines are provided as a guide to the eye).

treatment at a temperature of 780 °C, which is less than for HEBM single 1:12 phase $Nd_{12}Fe_{75}Mo_{13}N_x$ powder, which has a coercivity of 435 kA m⁻¹ [10].

The behaviour of the remanent magnetic polarization J_r and intrinsic coercivity jH_c for HEBM processed powders, annealed at 665 °C for 30 min, as a function of the volume fraction of magnetically soft $\alpha-Fe$ phase in $Nd_{12.6}Fe_{69.3}Co_{11.6}Zr_{0.5}B_6/\alpha-Fe$, is shown in Fig. 5. With an increasing volume fraction of

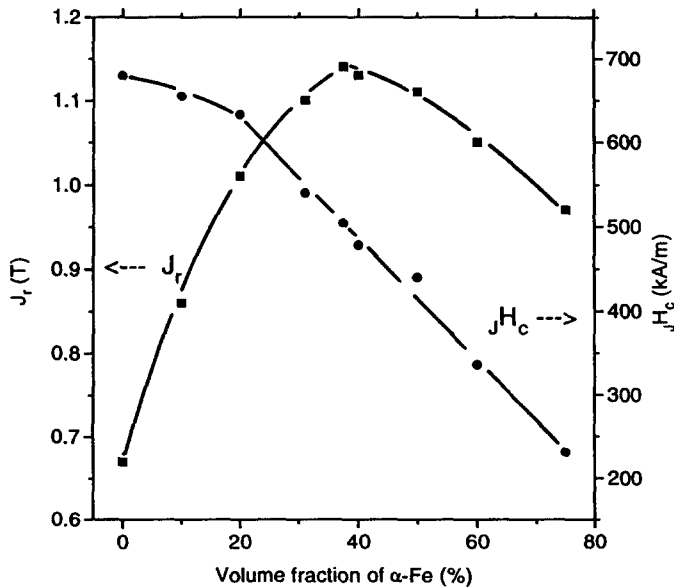


Fig. 5. The remanent polarization J_r and intrinsic coercivity jH_c of $Nd_{12.6}Fe_{69.3}Co_{11.6}Zr_{0.5}B_6/\alpha-Fe$ powders as a function of volume fraction of magnetically soft $\alpha-Fe$ phase content (lines are provided as a guide to the eye).

magnetically soft α -phase, the material shows an increase in J_r which passes through a maximum for 37.5–40% $\alpha-Fe$. The intrinsic coercivity decreases with increasing volume fraction of the magnetically soft $\alpha-Fe$ phase, from 680 kA m⁻¹ for 0% to 231 kA m⁻¹ for 75%.

Fig. 6 compares the hysteresis curves for HEBM and epoxy bonded $Nd_{12.6}Fe_{69.3}Co_{11.6}Zr_{0.5}B_6/\alpha-Fe$ and $Nd_{12.6}Fe_{81.4}B_6/\alpha-Fe$ powders for a 50% volume fraction of the magnetically soft $\alpha-Fe$ phase. The Co- and Zr-free $Nd_2Fe_{14}B$ -type powder has a lower remanent magnetization, lower intrinsic coercivity, and the reduced remanent magnetic polarization is less than 0.5. A good compromise between an enhanced J_r and an acceptable value for jH_c is obtained in $Nd_{12.6}Fe_{69.3}Co_{11.6}Zr_{0.5}B_6/\alpha-Fe$ powder, with a 37.5% volume fraction of $\alpha-Fe$, as it has a J_r of 1.14 T, jH_c of 504 kA m⁻¹ and α of 0.7, which compares with $J_r \approx 1.0$ T, $\alpha \approx 0.68$ and $jH_c \approx 477$ kA m⁻¹ reported by Gong et al. [5] for mechanically alloyed $(Nd,Tb)_2Fe_{14}B/(FeCo,FeNb)$ powders. The enhancement of J_r in the Zr containing material can be related to both a reduction in grain size of the soft magnetic $\alpha-Fe$ phase and an increase in the anisotropy due to zirconium additions [11].

The magnetic hysteresis curve for HEBM, annealed and nitrided $Nd_{12}Fe_{75}Mo_{13}/\alpha-Fe$ material with a volume fraction of magnetically soft $\alpha-Fe$ phase of 40% is shown in Fig. 7, and is compared with an $Nd_{12}Fe_{75}Mo_{13}N_x$ powder [10]. Exchange interaction between a soft magnetic $\alpha-Fe$ and a hard magnetic $Nd(Fe,Mo)_{12}N_x$ phase results in a significant enhance-

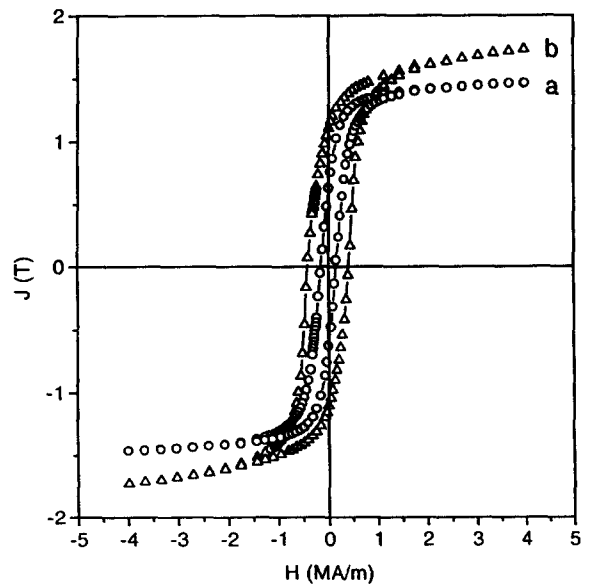


Fig. 6. Magnetic polarization J as a function of the applied field H for (a) $Nd_{12.6}Fe_{81.4}B_6/\alpha-Fe$ and (b) $Nd_{12.6}Fe_{69.3}Co_{11.6}Zr_{0.5}B_6/\alpha-Fe$ powders with a volume fraction of magnetically soft $\alpha-Fe$ phase of 50% (all data have been normalized to 100% density).

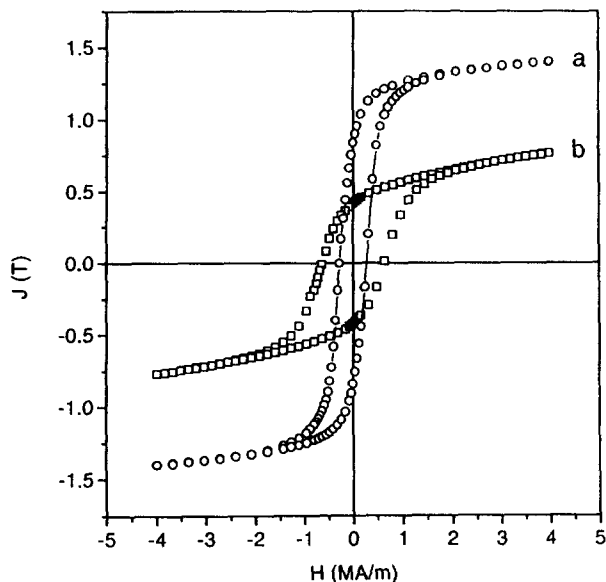


Fig. 7. Magnetic polarization J as a function of the applied field H for (a) $\text{Nd}_{12}\text{Fe}_{75}\text{Mo}_{13}\text{N}_x/\alpha\text{-Fe}$ powders with a volume fraction of magnetically soft $\alpha\text{-Fe}$ phase of 40% and (b) $\text{Nd}_{12}\text{Fe}_{75}\text{Mo}_{13}\text{N}_x$ (all data have been normalized to 100% density).

ment of the remanent magnetic polarization. Compared with $\text{Nd}(\text{Fe},\text{Mo})_{12}\text{N}_x$ powder, the $\text{Nd}(\text{Fe},\text{Mo})_{12}\text{N}_x/\alpha\text{-Fe}$ powder, with a volume fraction of magnetically soft $\alpha\text{-Fe}$ phase of 40%, has a lower coercivity, 281 kA m^{-1} compared with 716 kA m^{-1} , and a higher remanent magnetic polarization, 0.85 T compared with 0.42 T .

4. Conclusions

Remanence enhanced $\text{Nd}_2(\text{Fe},\text{Co},\text{Zr})_{14}\text{B}/\alpha\text{-Fe}$ and $\text{Nd}(\text{Fe},\text{Mo})_{12}\text{N}_x/\alpha\text{-Fe}$ powders, with a volume fraction of magnetically soft $\alpha\text{-Fe}$ phase of up to 75%, have been produced. The exchange coupled $\text{Nd}_2(\text{Fe},\text{Co},\text{Zr})_{14}\text{B}/\alpha\text{-Fe}$ magnet materials show a high remanent magnetic polarization of 1.14 T and an

intrinsic coercivity of 504 kA m^{-1} . Remanence enhanced $\text{Nd}(\text{Fe},\text{Mo})_{12}\text{N}_x/\alpha\text{-Fe}$ powders have also been produced. For $\text{Nd}_{12}\text{Fe}_{75}\text{Mo}_{13}\text{N}_x/\alpha\text{-Fe}$ powder, with a volume fraction of magnetically soft $\alpha\text{-Fe}$ phase of 40%, an intrinsic coercivity of 281 kA m^{-1} and a remanent magnetic polarization of 0.85 T have been obtained. $\text{Nd}_2(\text{Fe},\text{Co},\text{Zr})_{14}\text{B}/\alpha\text{-Fe}$ powders may be of potential use in the manufacture of polymer bonded magnets, because of their high J_r .

Acknowledgements

I thank Dr. S.J. Collocott for useful discussions and C. Andrikidis for assistance with the SQUID measurements. Support for this work was provided by the Australian Department of Industry, Science and Technology under the Generic Technology Component of the Industry Research and Development Act 1986.

References

- [1] R. Coehoorn, D.B. de Mooij and C. de Waard, *J. Magn. Magn. Mater.*, **80** (1989) 101.
- [2] E.F. Kneller and R. Hawig, *IEEE Trans. Magn.*, **27** (1991) 3588.
- [3] S. Hirosawa, H. Kanekiyo and M. Uehara, *J. Appl. Phys.*, **73** (1993) 6488.
- [4] A. Manaf, R.A. Buckley and H.A. Davies, *J. Magn. Magn. Mater.*, **128** (1993) 302.
- [5] W. Gong, G.C. Hadjipanayis and R.F. Krause, *J. Appl. Phys.*, **75** (1994) 6649.
- [6] T. Schrefl, J. Fidler and H. Kronmüller, *Phys. Rev. B* **49** (1994) 6100.
- [7] R. Skomski, *J. Appl. Phys.*, **76** (1994) 7059.
- [8] B.D. Cullity, *Elements of X-ray Diffraction*, Addison-Wesley, London, 1978, p. 102.
- [9] M. Jurczyk, J.S. Cook and S.J. Collocott, *J. Alloys Comp.*, **217** (1995) 65.
- [10] M. Jurczyk, P.B. Gwan and S.J. Collocott, *J. Alloys Comp.*, **221** (1995) 114.
- [11] M. Jurczyk and W.E. Wallace, *J. Magn. Magn. Mater.*, **59** (1986) L182.